eLIFE elifesciences.org

RESEARCH ARTICLE

Figures and figure supplements

Structure and *in situ* organisation of the *Pyrococcus furiosus* archaellum machinery

Bertram Daum *et al*

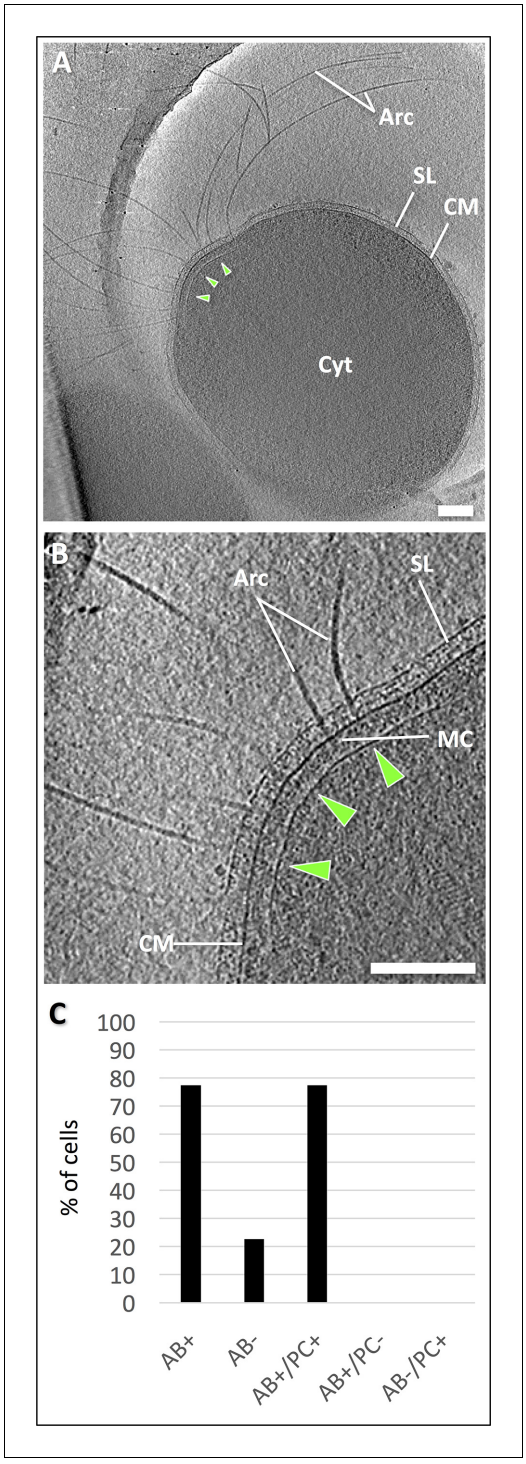

Figure 1. Electron cryo-tomography of *P. furiosus*. (**A**) tomographic slice through a frozen-hydrated *P. furiosus* cell. Arc, archaella; SL, S-layer; CM, cell membrane; Cyt, cytosol; green arrowheads, polar cap. (**B**) close-up of the tomogram in A, showing archaella on the cell pole. MC, motor complex. Scale bars, 200 nm. (**C**) percentage of total archaellar bundles observed as well as archaellar bundles observed with and without a polar cap.

Figure 1 continued on next page

Figure 1 continued

DOI: 10.7554/eLife.27470.002

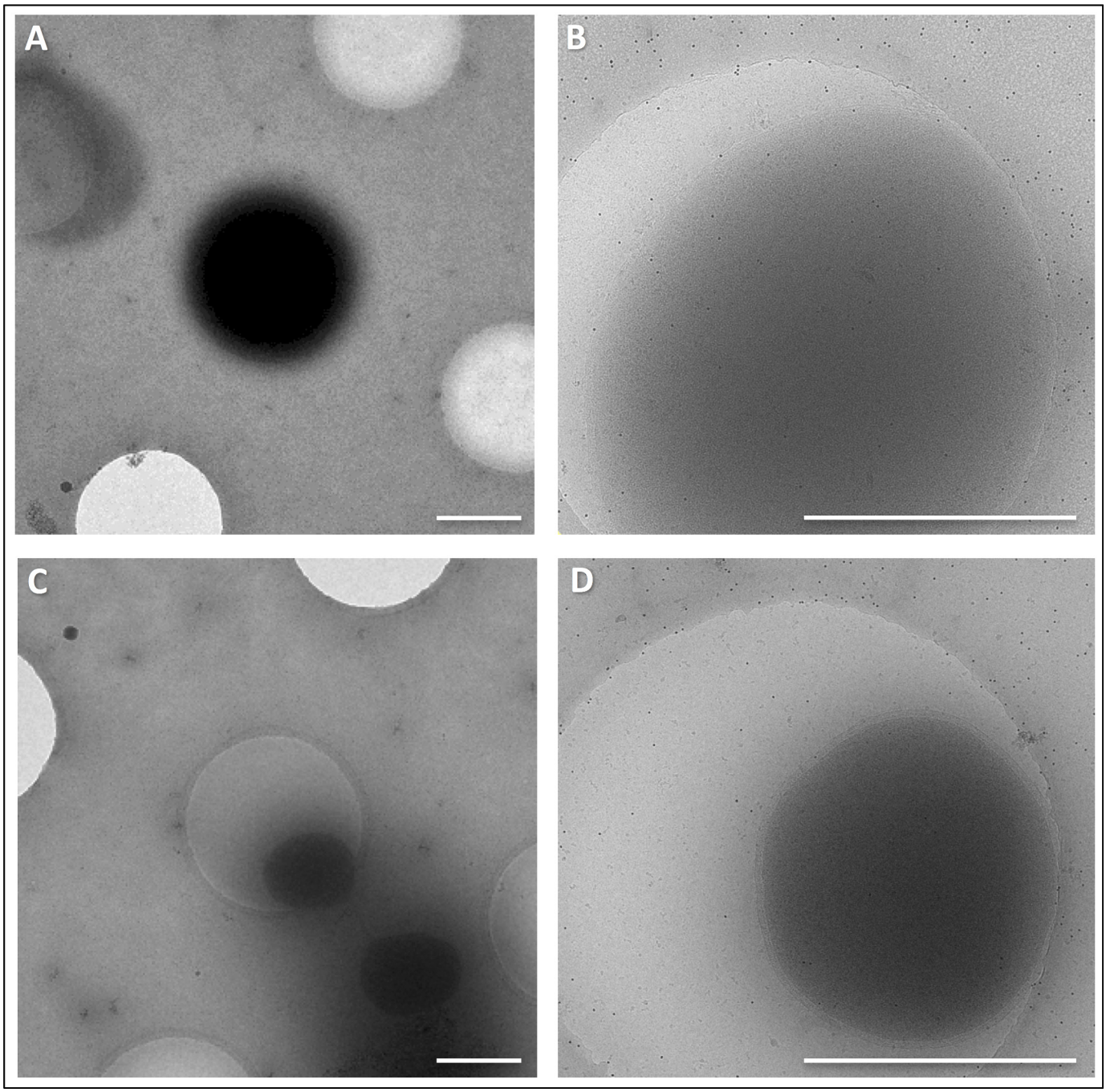

Figure 1—figure supplement 1. CryoEM of *P. furiosus* grown in full medium vs. pyruvate minimal medium. (**A** and **B**) cells grown in full medium at 5,600 x (A) and 41,000 x magnification (B). (C and D), cells grown in pyruvate minimal medium at 5,600 x (C) and 41,000 x magnification (D). Scale bars, 1 µm.

DOI: 10.7554/eLife.27470.003

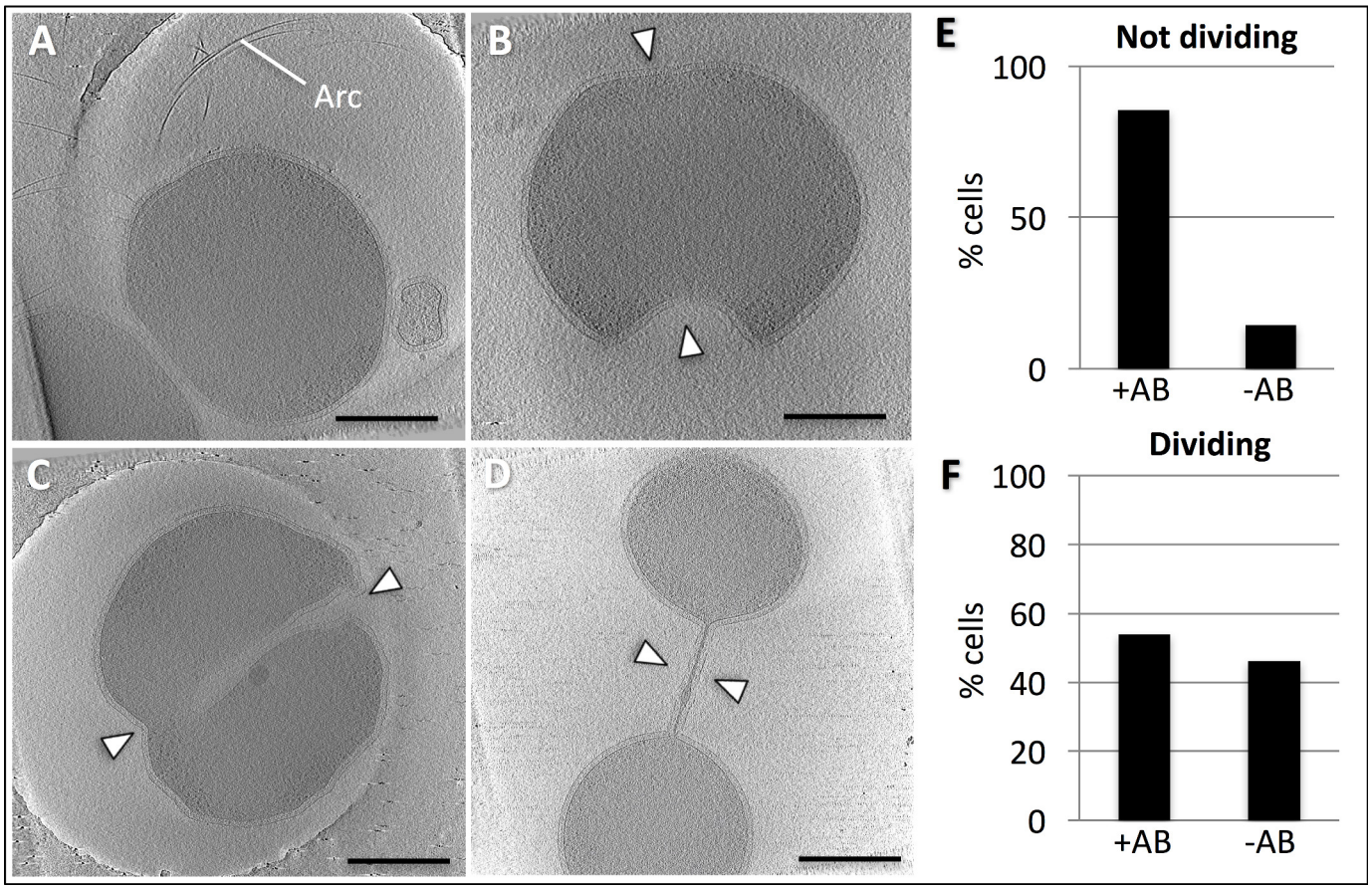

Figure 1—figure supplement 2. Tomographic slices of *P. furiosus* in different putative division states. (**A**) non-dividing (i.e. just divided); (**B**), early division; (**C**), intermediate division state; (**D**), late division state. Arc, archaella. Arrowheads indicate invagination. (**E**,**F**), frequency of observed archaella in dividing (**E**) and non-dividing (**F**) cells. Scale bars, 500 nm.

DOI: 10.7554/eLife.27470.004

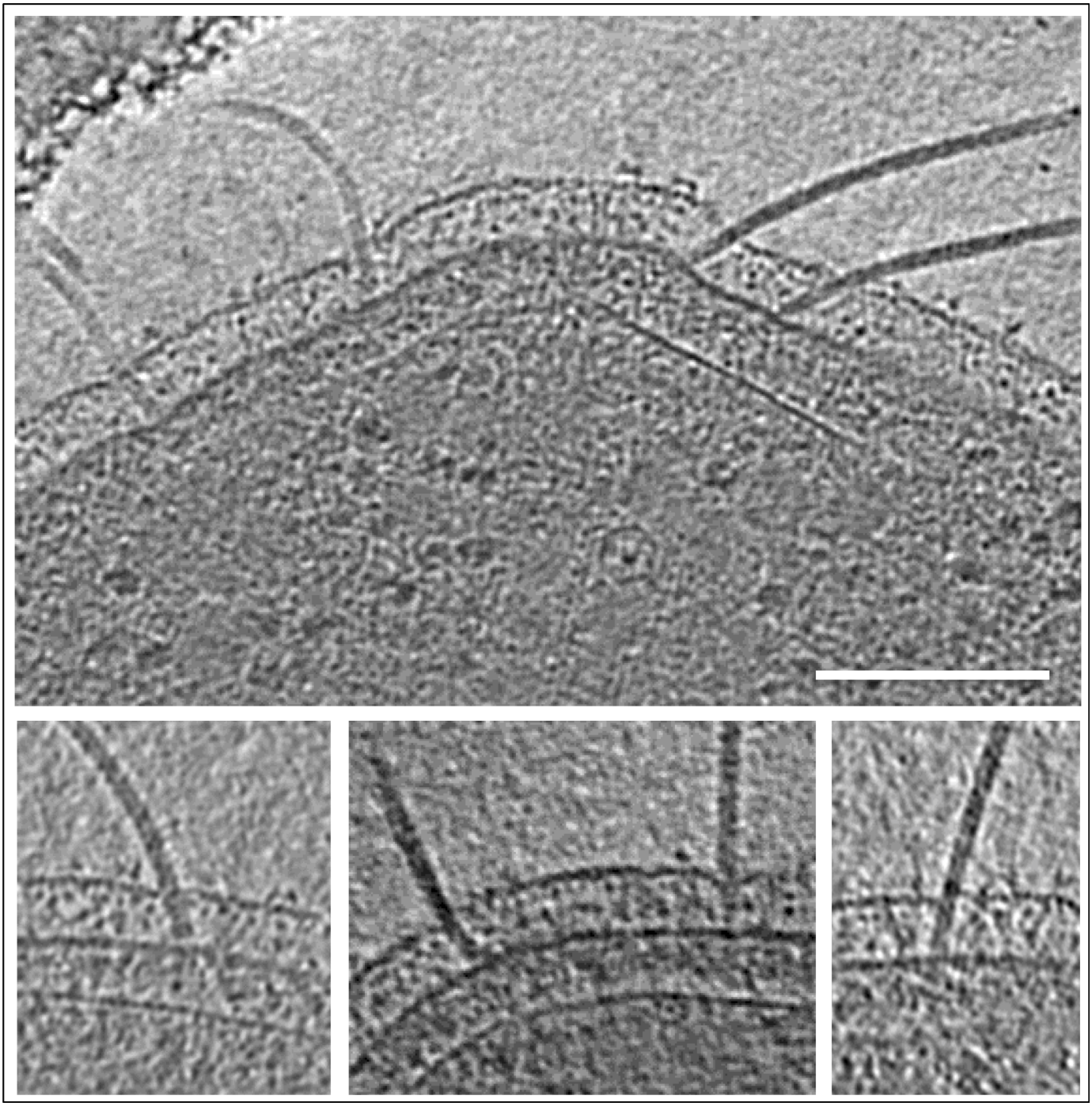

Figure 1—figure supplement 3. Angular freedom of archaella in the periplasm. Panels show different close-ups of slices though tomograms of frozen-hydrated *P. furiosus* cells. Scale bar, 100 nm.
DOI: 10.7554/eLife.27470.005

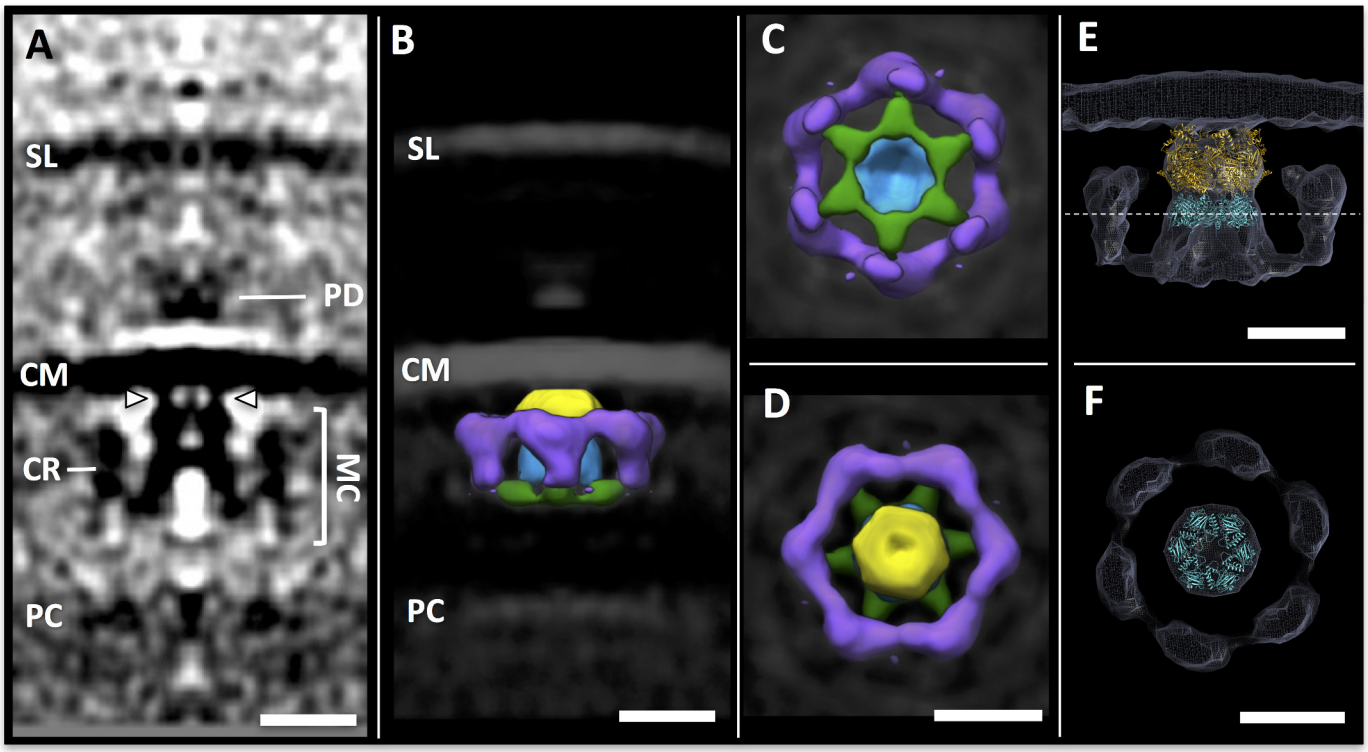

Figure 2. Sub-tomogram averaging of the archaellar motor complex. (**A**) tomographic slice through the sub-tomogram average of the motor complex. SL, S-layer; PD; periplasmic densities; CM, cell membrane; MC, motor complex; CR, cytosolic ring; PC, polar cap. Arrowheads indicate two of six narrow connections between MC and CM. (**B–D**) segmented 3D surface representation of the sub-tomogram average of the MC (multiple colours) as seen from the side (**B**), the cytosol (**C**) and the cell membrane (**D**). Yellow, blue, green, central complex; purple, cytosolic ring. (**E,F**) *S. acidocaldarius* FlaI (PDB-4IHQ, gold) and Symmdoc model of *S. acidocaldarius* FlaH (PDB-4YDS, cyan) fitted into the MAC density in side view (**E**) and in cross-section through FlaH (**F**); position of cross-section shown as dotted line in E. Scale bars, 20 nm.

DOI: 10.7554/eLife.27470.006

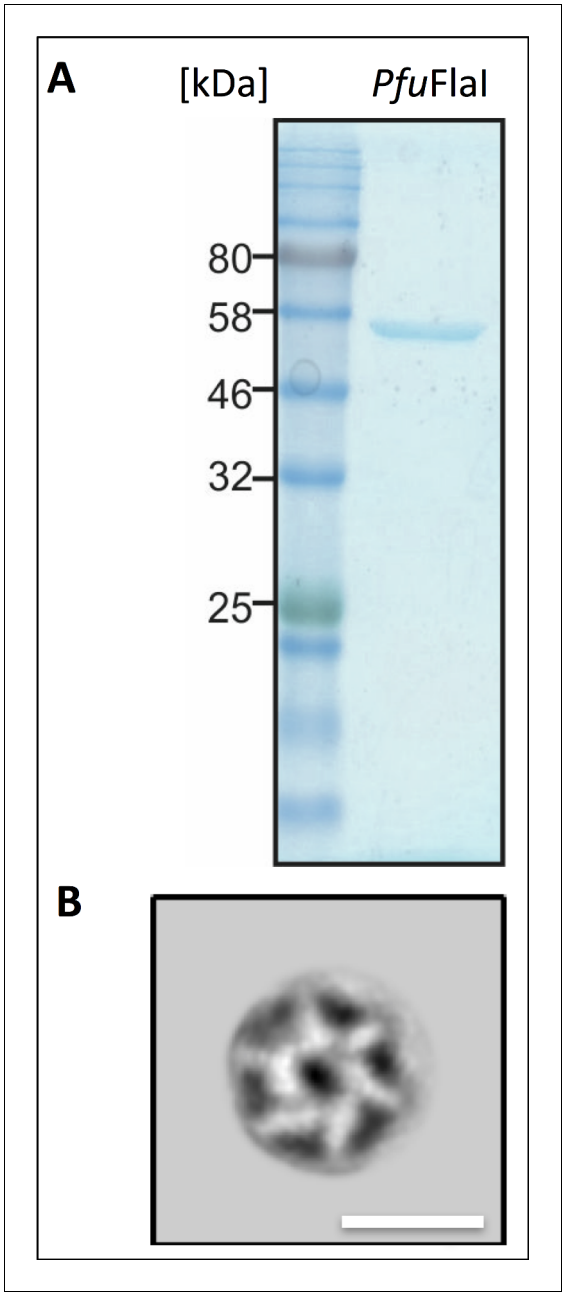

Figure 2—figure supplement 1. Purification and negative stain EM of *P. furiosus* FlaI. (**A**) SDS gel of FlaI peak fraction after gel filtration chromatography. Stained with Coomassie Brilliant Blue. Marker: Thyroglobulin (669 kDa), γ globulin (158 kDa), ovalbumin (44 kDa), myoglobin (17 kDa) and vitamin B12 (1.35 kDa). (**B**) projection map obtained from 2D classification of negatively stained FlaI. Note that protein density is white. Scale bar, 15 nm.
DOI: 10.7554/eLife.27470.007

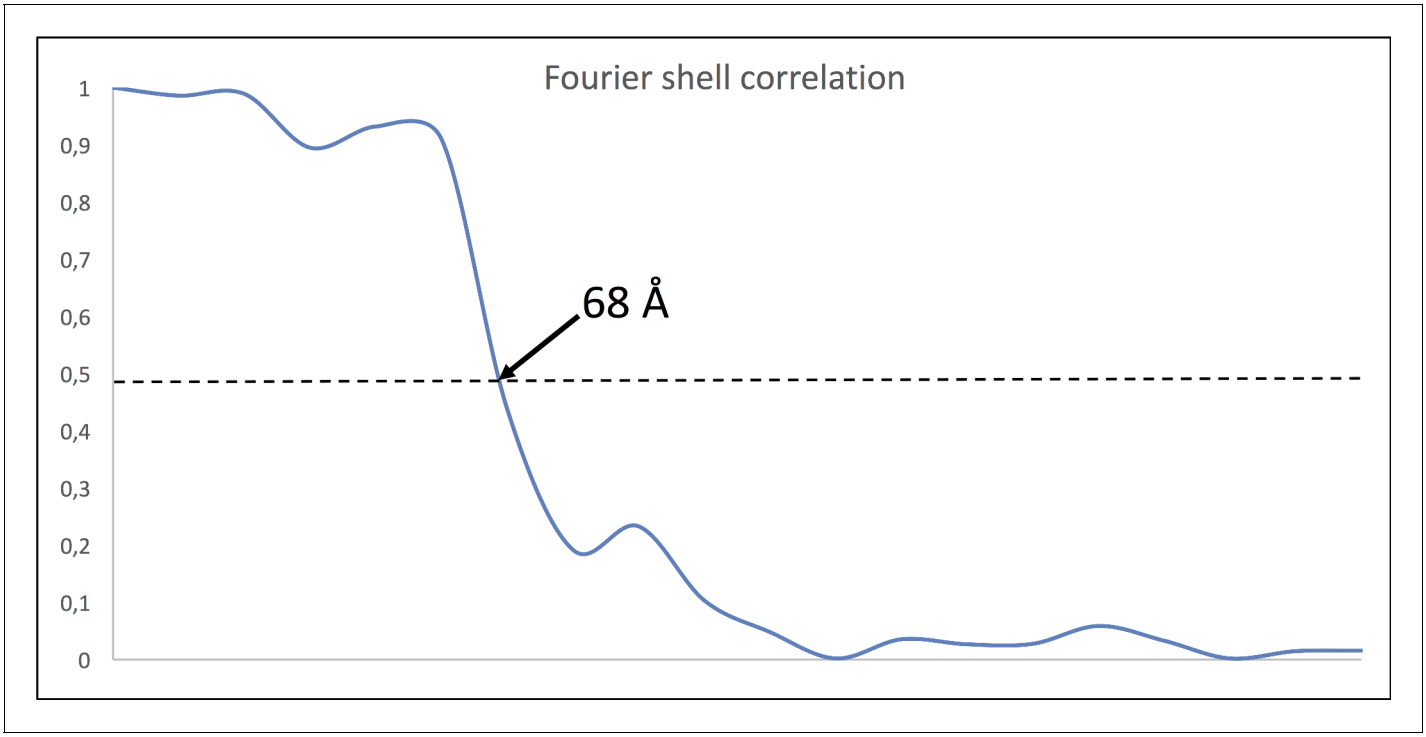

Figure 2—figure supplement 2. Fourier Shell Correlation (FSC) of MC sub-tomogram average. FSC of two half maps of 2,274 (379 × 6) particles indicates a resolution of ~68 Å using the 0.5 criterion.
DOI: 10.7554/eLife.27470.008

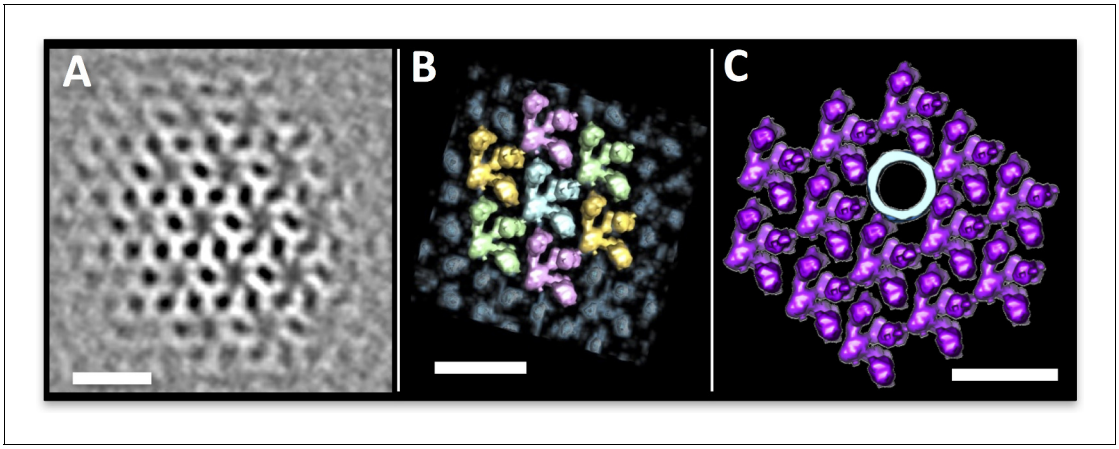

Figure 3. The *P. furiosus* S-layer. (**A–C**) sub-tomogram averaging of the *P. furiosus* S-layer as tomographic slice (**A**), segmented 3D surface representation with asymmetric units in different colours (**B**) and one subunit replaced by a 3D surface-rendered sub-tomogram of a *P. furiosus* archaellum (**C**; purple, S-layer; light blue, archaellum). Scale bars, 20 nm.
DOI: 10.7554/eLife.27470.009

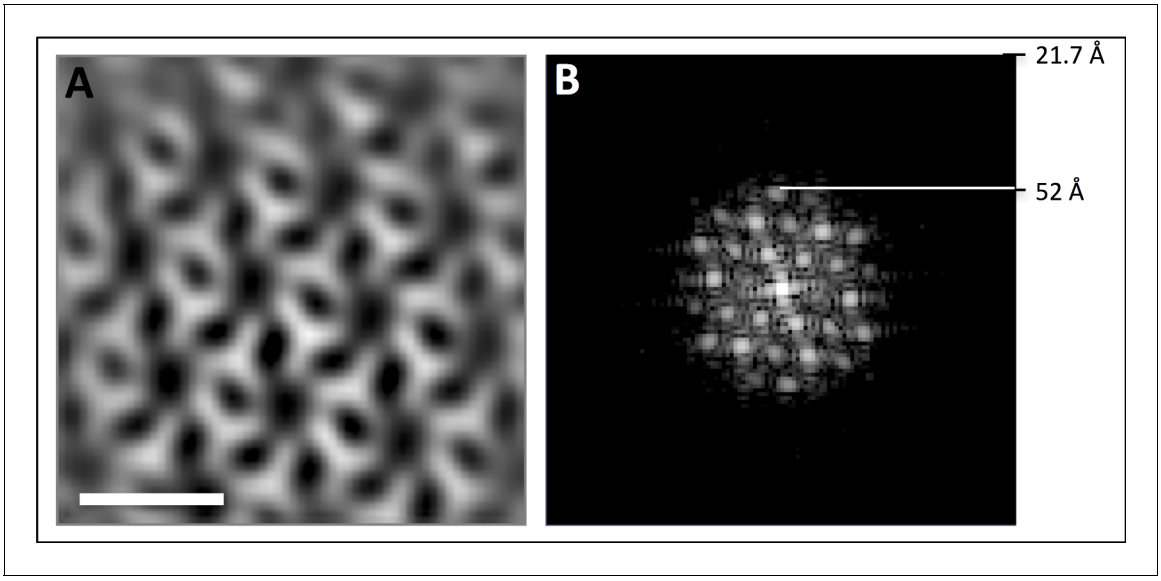

Figure 3—figure supplement 1. - Resolution estimate of *P. furiosus* S-layer sub-tomogram average. (**A**) tomographic slice through S-layer average. (**B**) power spectrum of A showing diffraction up to 52 Å. Nyquist at 21.7 Å. Scale bar, 20 nm.
DOI: 10.7554/eLife.27470.010

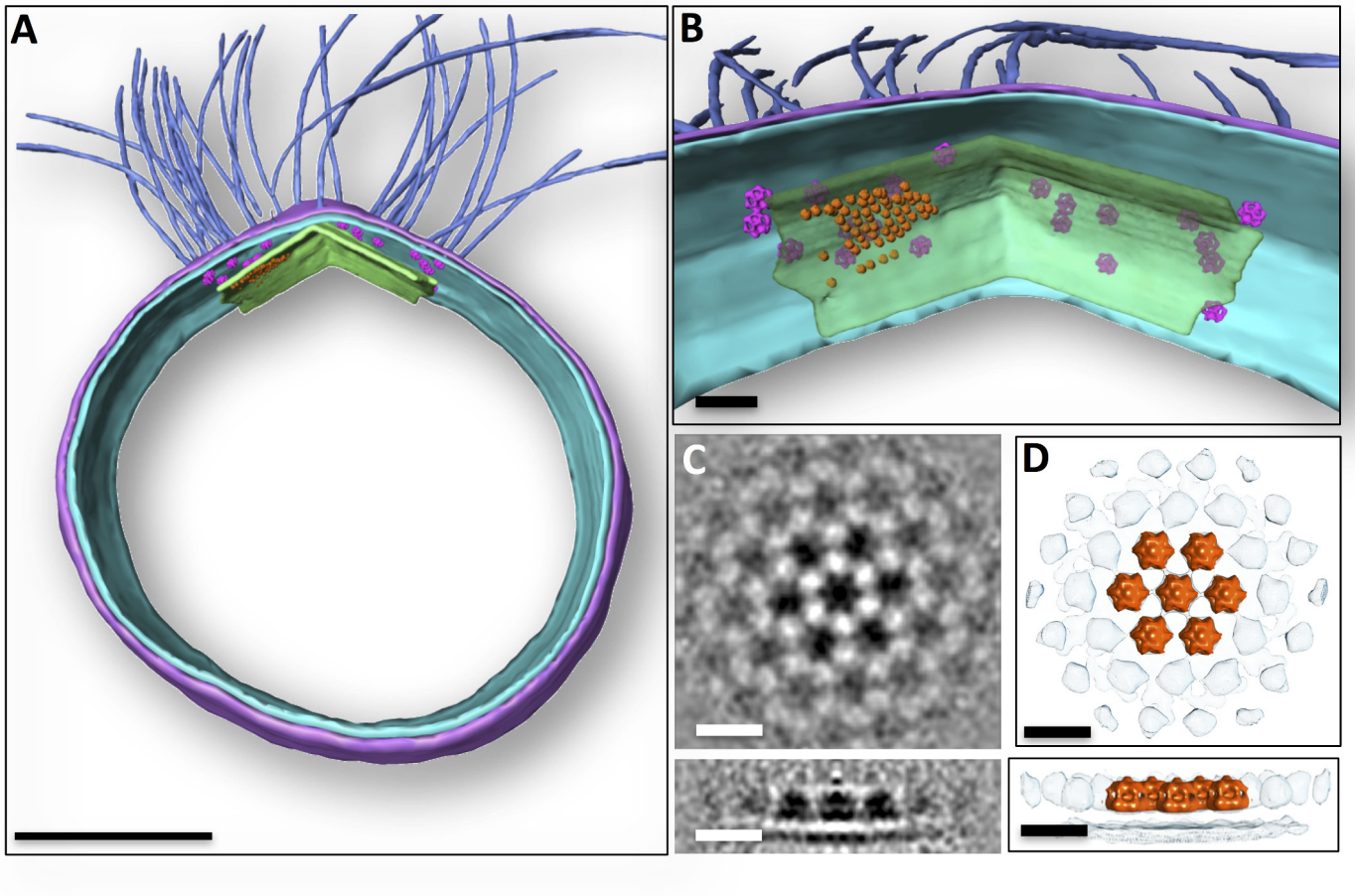

Figure 4. Subcellular organisation of motor complexes and polar cap. (**A**) Segmented 3D representation of a tomogram of a *P. furiosus* cell. Motor complexes (magenta) have been repositioned into the original tomogram using coordinates from sub-tomogram averaging. Medium blue, archaella; purple, S-layer; cyan, cell membrane; green, polar cap. (**B**) close-ups of the polar region showing layer-like superimposition of motor complexes, polar cap and hexagonal protein array (orange). Note that due to limitations of manual particle picking only subsets of the motor complexes and hexagonal protein arrays are displayed. (**C** and **D**) sub-tomogram average of hexameric protein array associated with polar cap as slices through the average (**C**), as well as segmented surface representation (**D**) in top (top panel) and side view (bottom panel). Scale bars, 200 nm (**A**); 50 nm (**B**); 15 nm (**C, D**).
DOI: 10.7554/eLife.27470.011

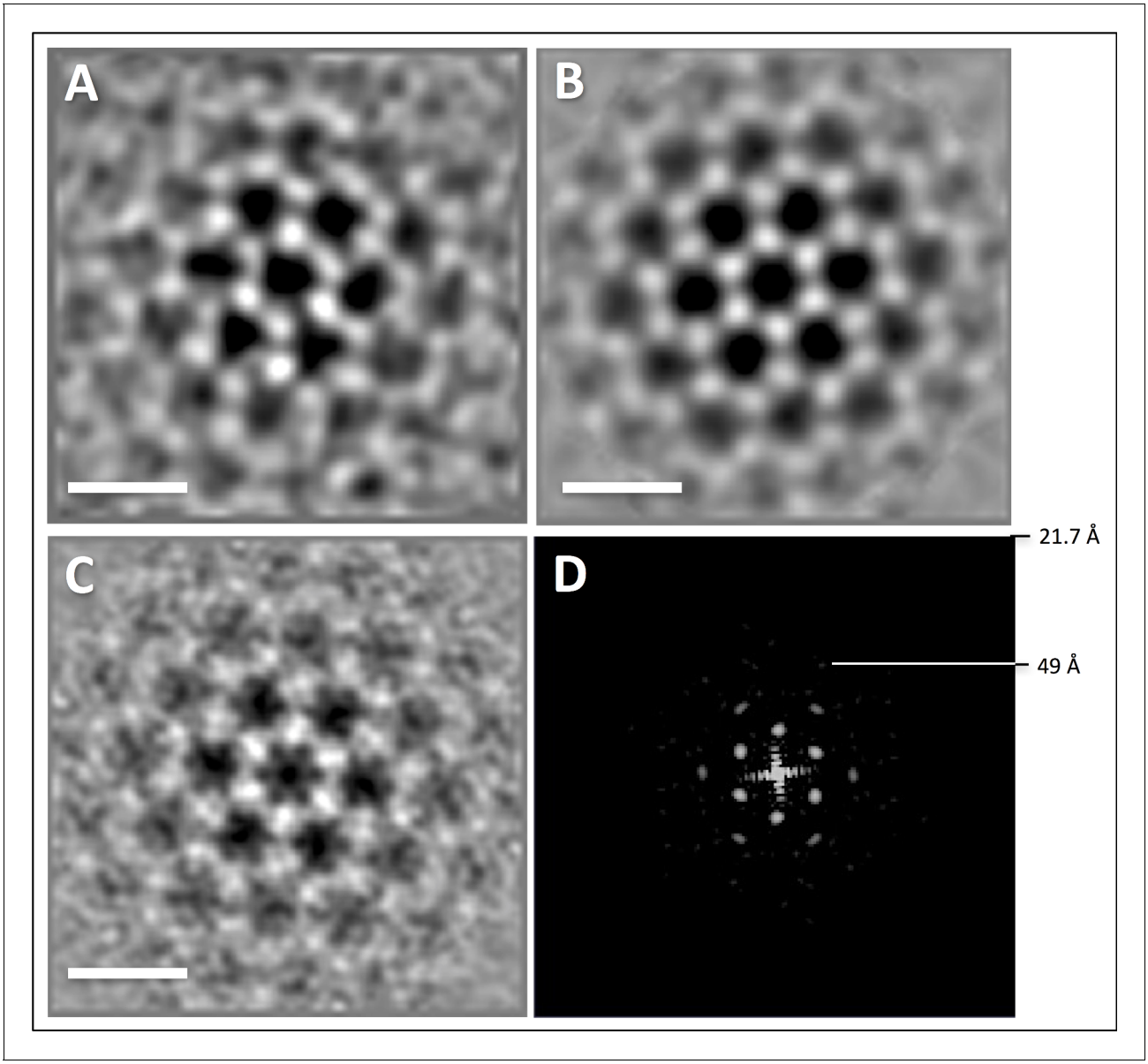

Figure 4—figure supplement 1. Sub-tomogram averaging and resolution of hexagonal protein array. (**A**) average filtered with nonlinear anisotropic diffusion indicating hexagonal symmetry of the array. (**B**) average from A with 6-fold symmetry applied. (**C**), average of unfiltered sub-volumes with 6-fold symmetry applied. (**D**) power spectrum of C showing diffraction up to 49 Å. Nyquist at 21.7 Å. Scale bars, 20 nm.
DOI: 10.7554/eLife.27470.012

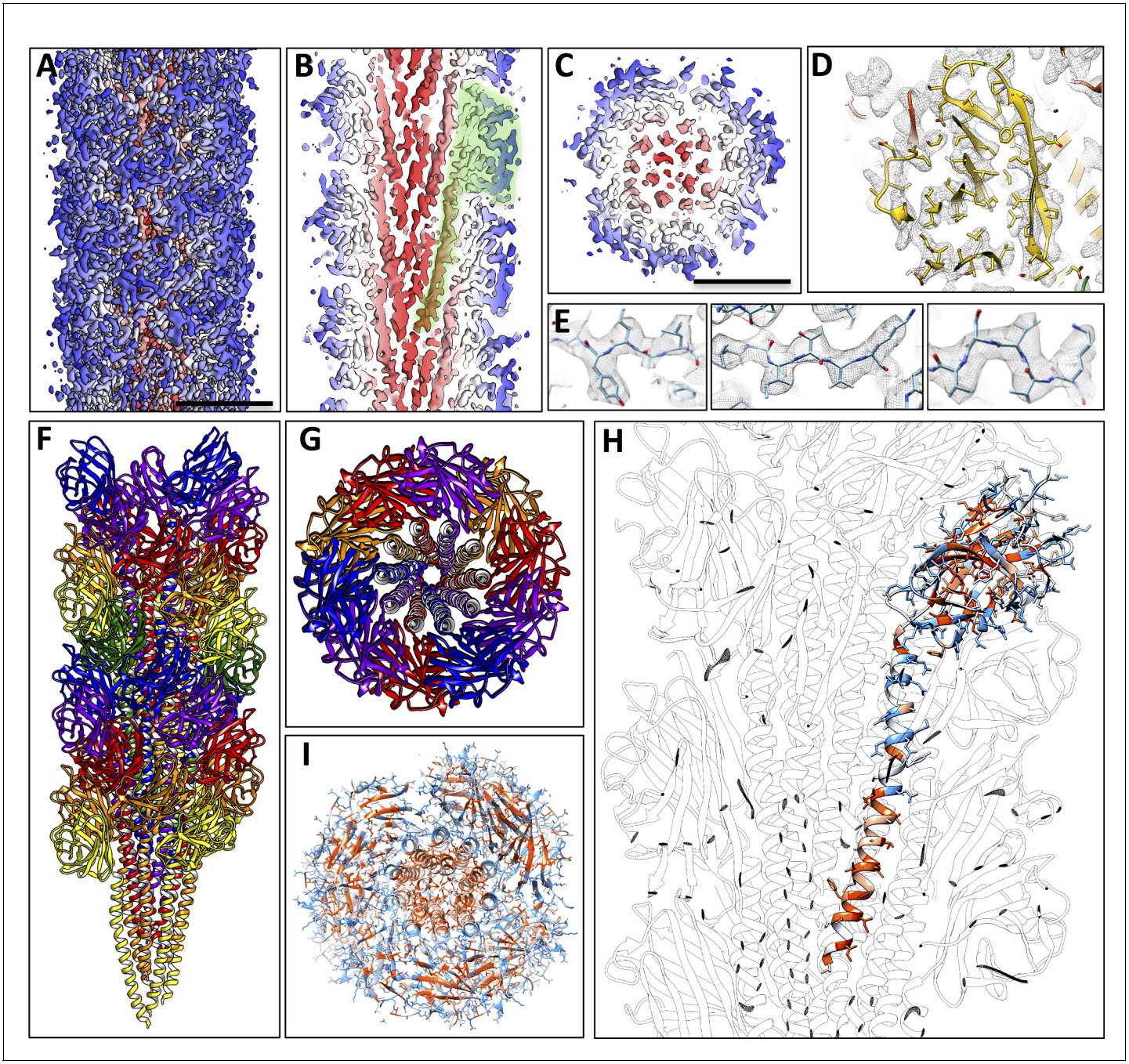

Figure 5. Structure of the *P. furiosus* archaellum. (**A–C**) 3D representation of the 4.2 Å map of the *P. furiosus* archaellum as seen from the surface (**A**), and cross-sections parallel (**B**) and perpendicular (**C**) to the long axis of the filament. Different colours represent different regions of the archaellum; red, inner helix bundle; white – blue, outer beta-strand-rich sheath; transparent green, outline of one archaellin monomer. Scale bars A, C, 50 Å. (**D**) Slice through the outer sheath of the filament showing the β-strand rich region of the $FlaB_0$ monomer (yellow) fitted into the map density (transparent grey). Note hydrophobic amino acid side chains pack in the interior of the β-barrel. (**E**) Close-ups of beta strands of $FlaB_0$ (backbone in blue) fitted into the map density (transparent grey). (**F, G**) Side view (**F**) and cross-section (**G**) of the atomic model of the *P. furiosus* archaellum with individual $FlaB_0$ subunits in different colours. (**H**) structure of the $FlaB_0$ monomer coloured by hydrophobicity (red, hydrophobic; blue, hydrophilic). Neighbouring subunits within the filament are shown in transparent grey. (**I**) structure of the *P. furiosus* archaellum coloured by hydrophobicity in top view.

DOI: 10.7554/eLife.27470.013

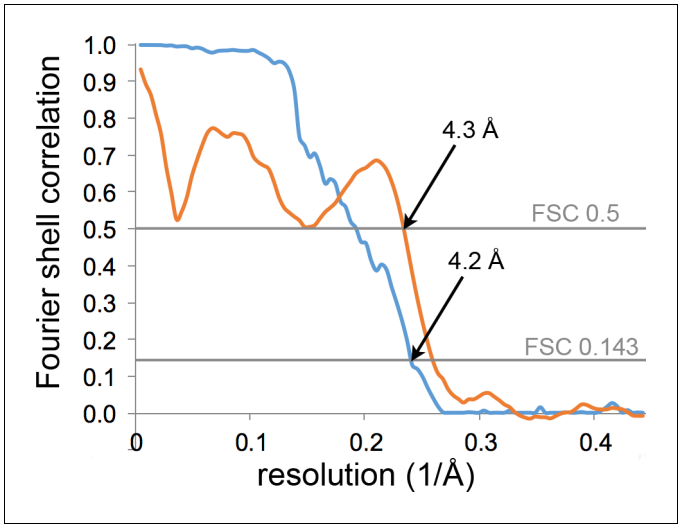

Figure 5—figure supplement 1. Resolution estimation and model validation of the *P. furiosus* archaellum. Gold-standard Fourier shell correlation (FSC) of the map after masking as determined by the post-processing procedure in RELION (blue) and FSC between the map and the final model (orange).
DOI: 10.7554/eLife.27470.014

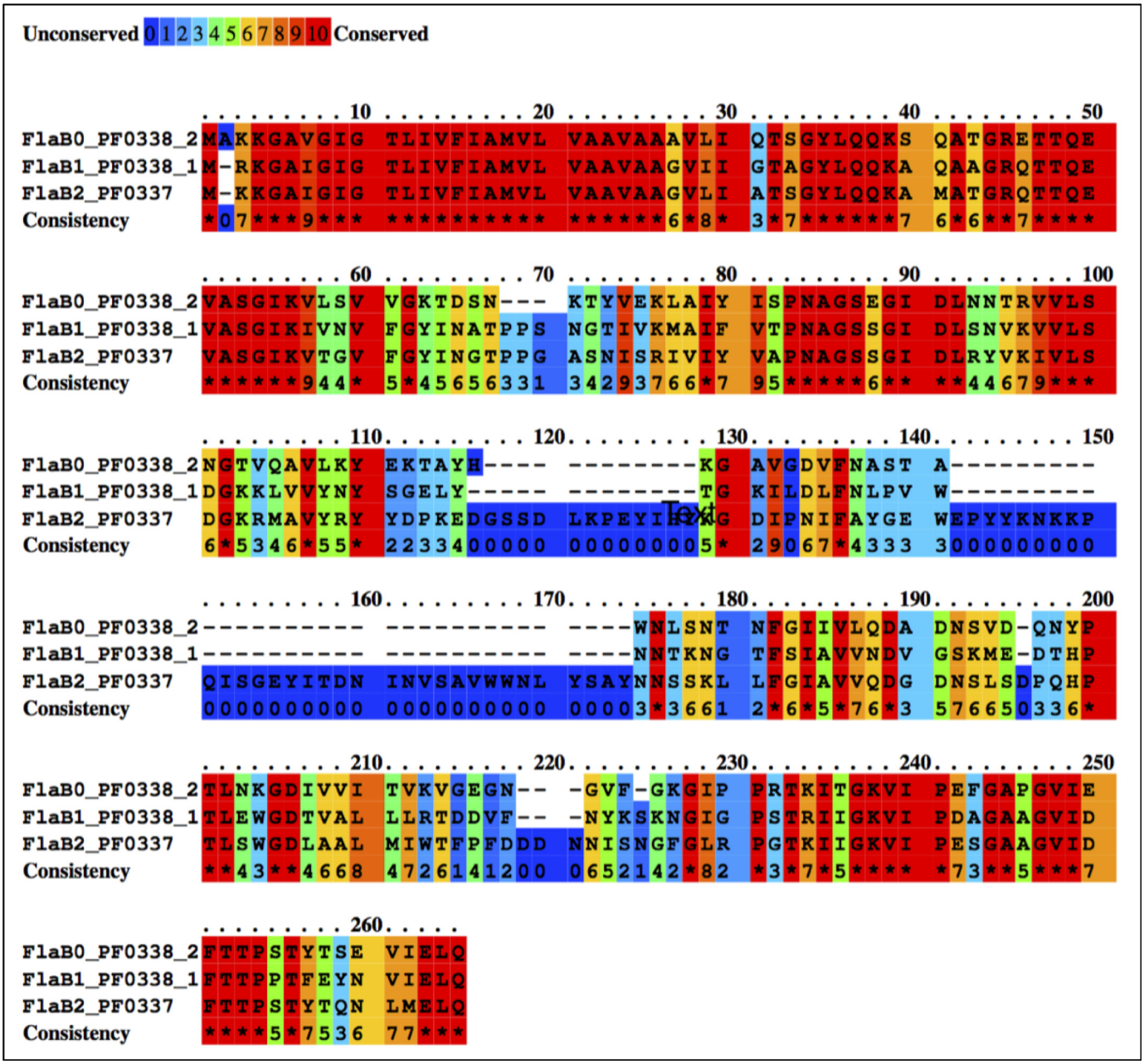

Figure 5—figure supplement 2. Multiple sequence alignment between *P. furiosus* $FlaB_0$, $FlaB_1$ and $FlaB_2$ using the Praline server (http://www.ibi.vu.nl/programs/pralinewww/), showing sequence conservation.

DOI: 10.7554/eLife.27470.015

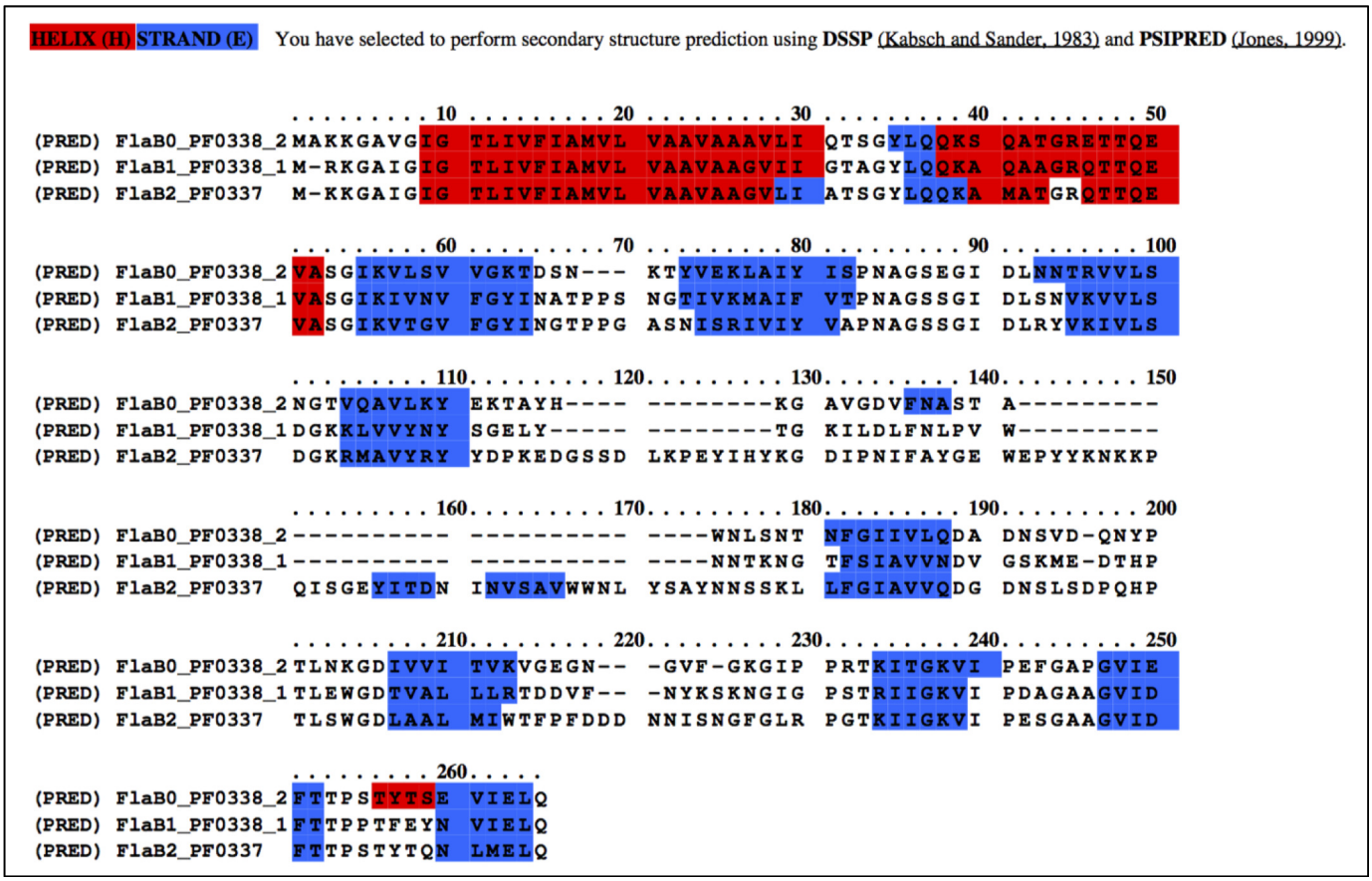

Figure 5—figure supplement 3. Multiple sequence alignment of *P. furiosus* $FlaB_0$, $FlaB_1$ and $FlaB_2$ using the Praline server (http://www.ibi.vu.nl/programs/pralinewww/), showing secondary structure prediction (helices, red; beta strands, blue).
DOI: 10.7554/eLife.27470.016

```
# WEBSEQUENCE Length: 212
# WEBSEQUENCE Number of predicted TMHs:  1
# WEBSEQUENCE Exp number of AAs in TMHs: 22.90416
# WEBSEQUENCE Exp number, first 60 AAs:  22.88168
# WEBSEQUENCE Total prob of N-in:        0.96086
# WEBSEQUENCE POSSIBLE N-term signal sequence
WEBSEQUENCE     TMHMM2.0        inside       1     6
WEBSEQUENCE     TMHMM2.0        TMhelix      7    29
WEBSEQUENCE     TMHMM2.0        outside     30   212
```

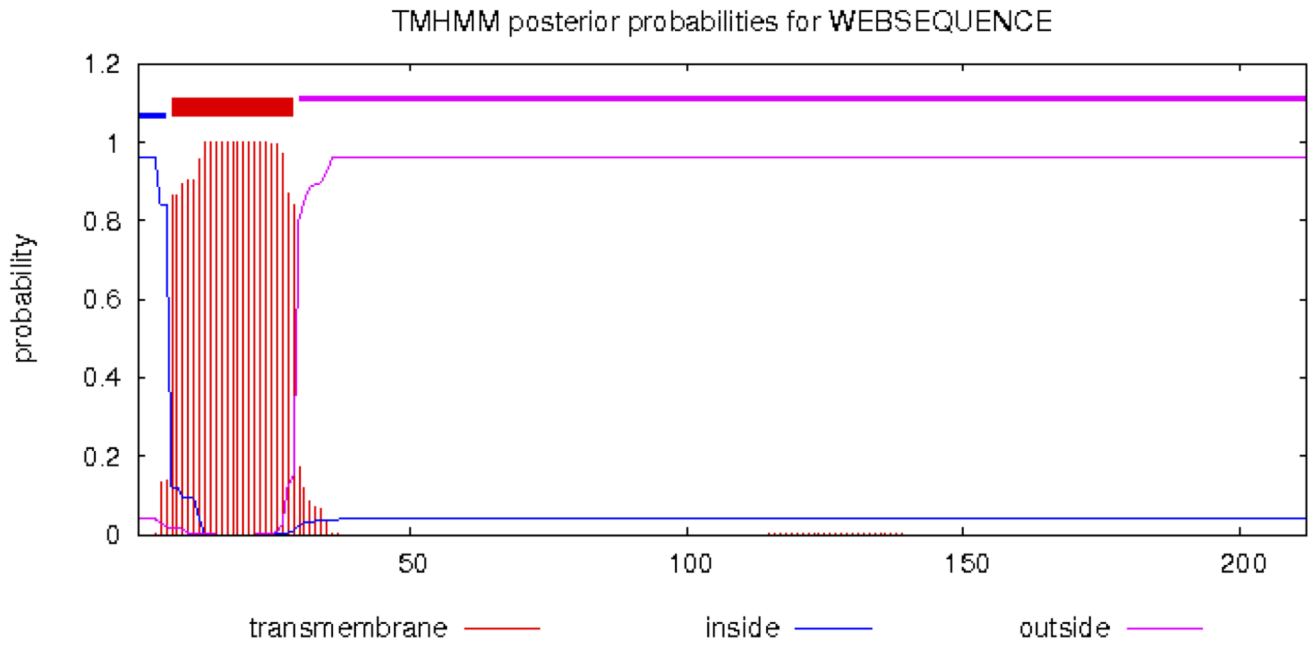

Figure 5—figure supplement 4. Transmembrane helix prediction of *P. furiosus* $FlaB_0$ using the TMHMM server (http://www.cbs.dtu.dk/services/TMHMM/) predicting residues 1–6 inside, 7–29 as transmembrane helix and 30–212 outside (periplasm).
DOI: 10.7554/eLife.27470.017

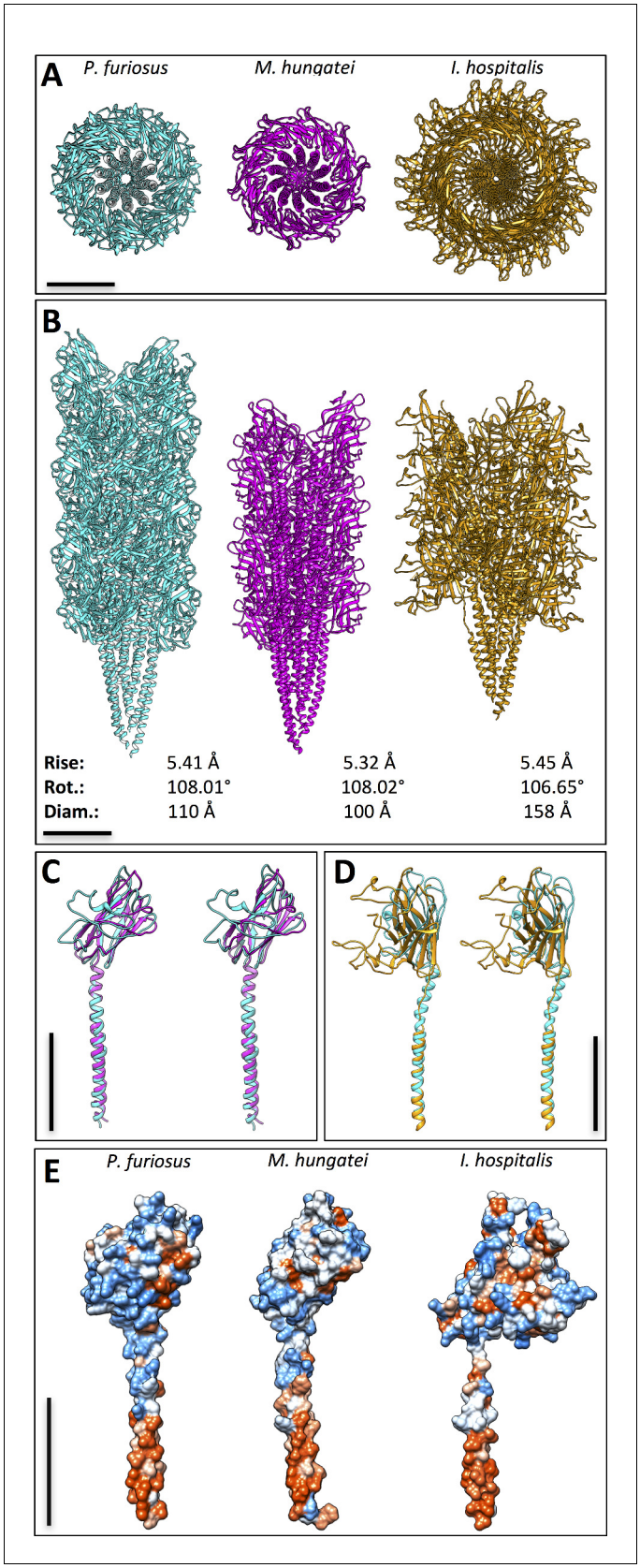

Figure 5—figure supplement 5. Comparison between three archaeal filaments. Structures of archaella from *Pyrococcus furiosus* (cyan) and *Methanospirillum hungatei* (magenta), as well as *Iho*670 fiber from *Ignicoccus*

Figure 5—figure supplement 5 continued on next page

Figure 5—figure supplement 5 continued

hospitalis (gold) in top (**A**) and side (**B**) views. Helical parameters rise and rotation (rot.), as well as diameters (diam.) are indicated. (**C**) overlay of *Pfu*FlaB$_0$ (cyan) and *Mhu*FlaB$_3$ (magenta) in stereo view. (**D**) overlay of *Pfu*FlaB$_0$ (cyan) and *Iho*670 (gold) in stereo view. (**E**) hydrophobicity surfaces of *Pfu*FlaB$_0$, *Mhu*FlaB$_3$ and *Iho*670; red, hydrophobic; blue, hydrophilic. Scale bars, 50 Å.

DOI: 10.7554/eLife.27470.018

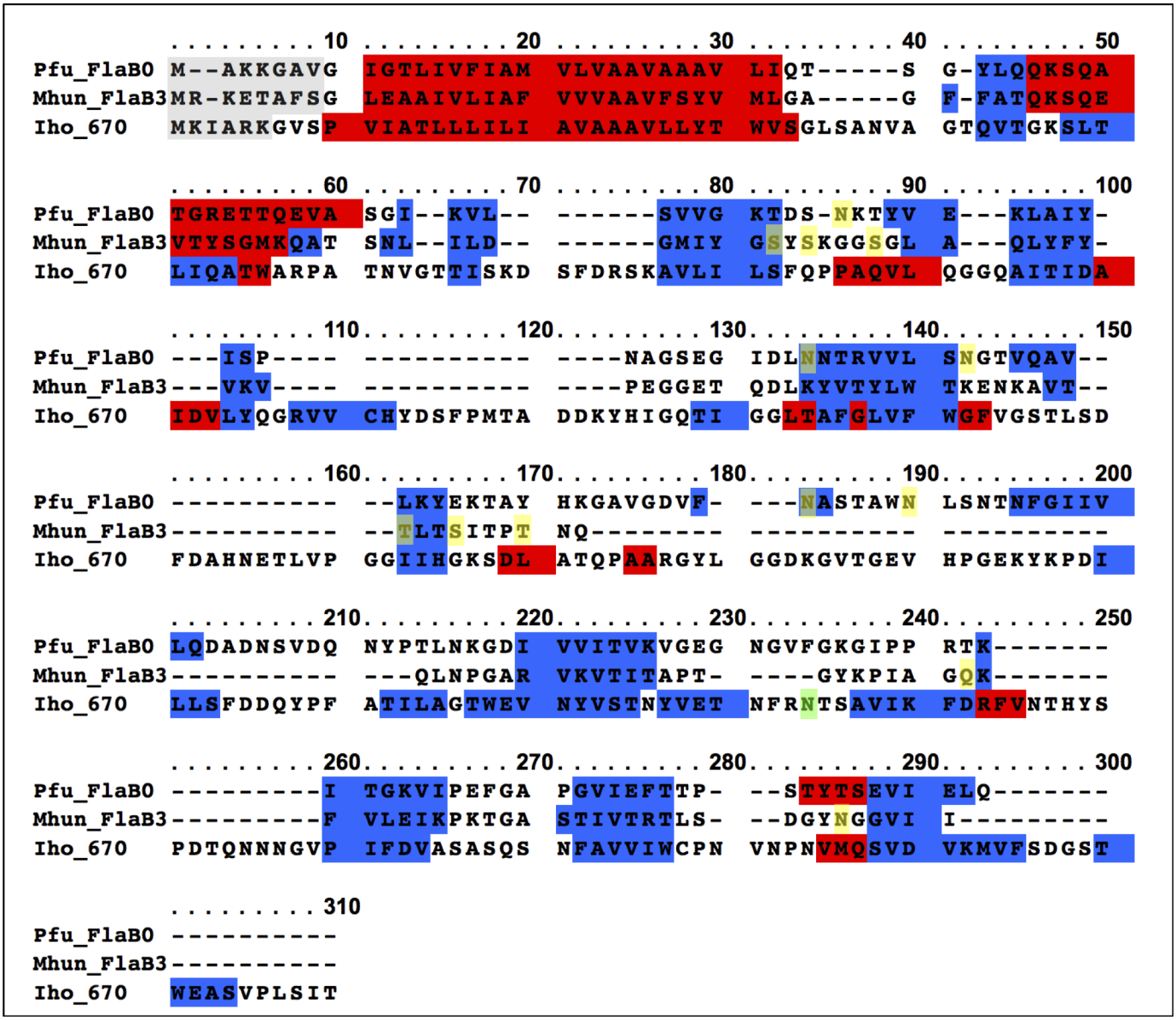

Figure 5—figure supplement 6. Sequence alignment of *P. furiosus* $FlaB_0$, *M. hungatei* $FlaB_3$ and the *I. hospitalis* 670 polypeptides. Transparent grey, clipped signal peptide; red, predicted α-helix; blue, predicted beta-strand; yellow, experimentally determined N-and O-glycosylation sites in *P. furiosus* and *M. hungatei*; green, singular putative N-glycosylation site in *I. hospitalis*.

DOI: 10.7554/eLife.27470.019

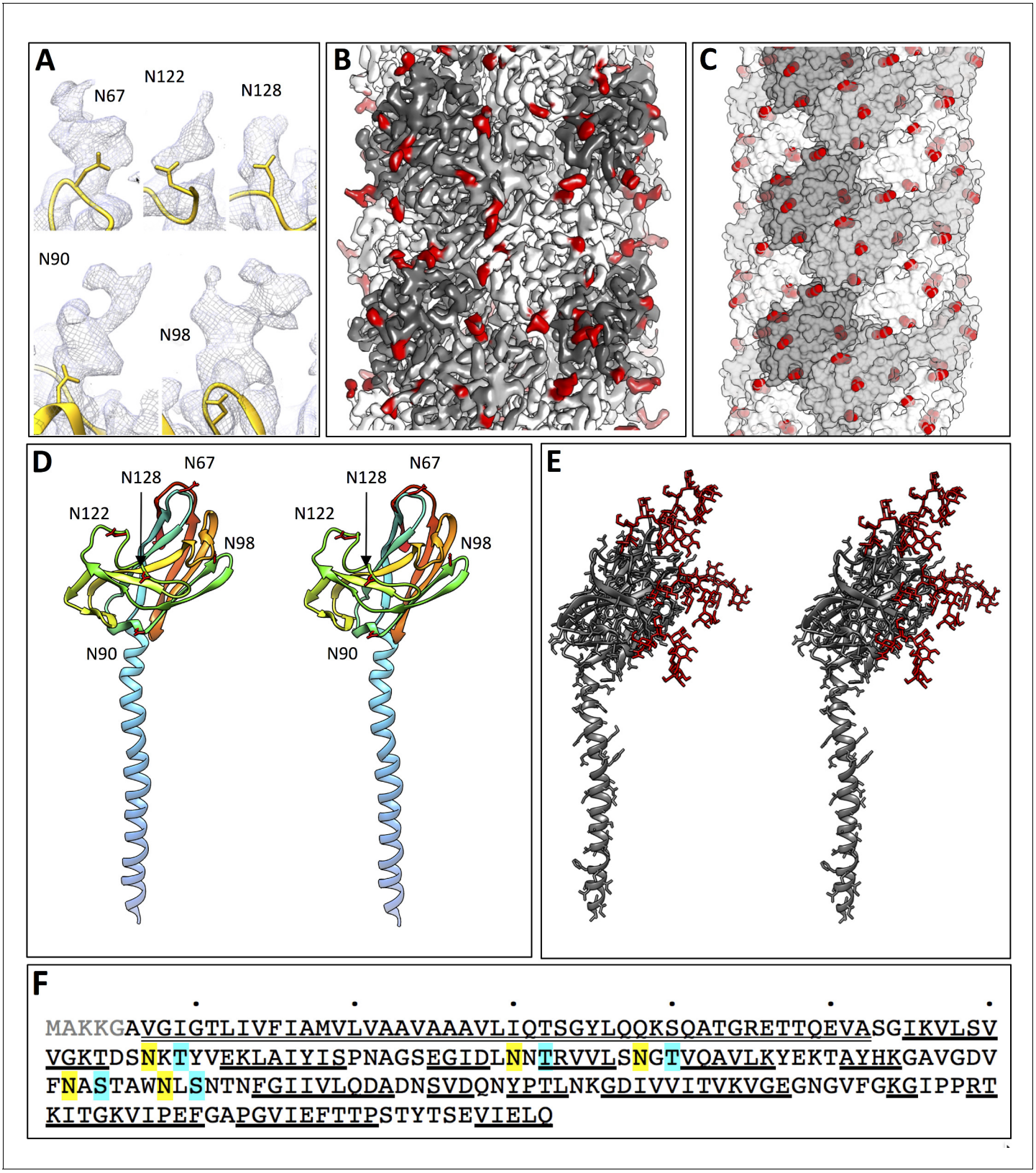

Figure 6. Glycosylation of the *P. furiosus* archaellum. (**A**) Close-ups of glycan densities near Asn residues. (**B**) surface representation of EM map showing glycan densities (red) protruding from the filament (shades of grey). (**C**) Surface representation of the atomic model of the archaellum (shades of grey, individual $FlaB_0$ subunits; red, asparagine residues within glycosylation sequon). (**D**) stereo view of the *P. furiosus* $FlaB_0$ monomer in rainbow

Figure 6 continued on next page

Figure 6 continued

representation (blue, N-terminus; red, C-terminus) with glycosylated asparagines labelled in red. (**E**) stereo view of the *P. furiosus* $FlaB_0$ monomer (dark grey) and glycan structures (red) modelled near glycosylated Asn residues. (**F**) sequence of *P. furiosus* $FlaB_0$. Grey, clipped signal peptide; double line, α-helix; single line, β strand; yellow, glycosylated asparagine; blue, T/S residue in conserved glycosylation sequon; every 10^{th} residue of the *P. furiosus* sequence labelled by a dot.

DOI: 10.7554/eLife.27470.021

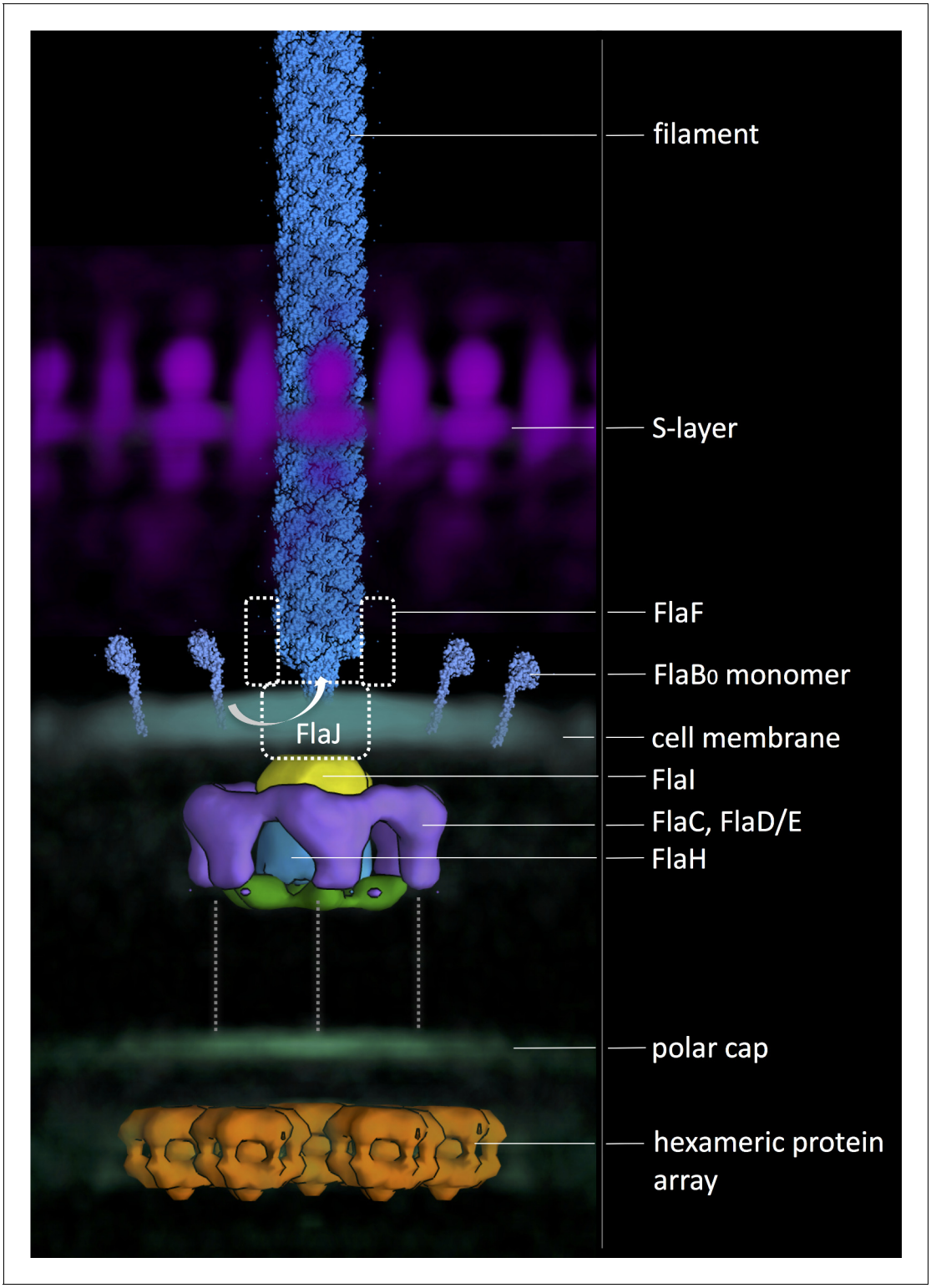

Figure 7. Composite model of the archaellum machinery of *P. furiosus*. Light blue, $FlaB_0$ monomers and filament (from helical reconstruction); hazy magenta, S-layer; solid yellow, blue, green and purple, motor complex; hazy blue, cell membrane; hazy green, polar cap; solid orange, hexagonal protein array (from different sub-tomogram averages). Putative positions of protein subunits are indicated. Dashed grey lines, putative interaction with polar cap.

DOI: 10.7554/eLife.27470.022